

## Orientation-Induced Crystallization in Isotactic Polypropylene Melt by Shear Deformation

R. H. Somani<sup>1</sup>, L. Yang<sup>1</sup>, I. Sics<sup>1</sup>, B. S. Hsiao<sup>1,\*</sup>, N. V. Pogodina<sup>2,+</sup>,  
H. H. Winter<sup>2</sup>, P. Agarwal<sup>3</sup>, H. Fruitwala<sup>3</sup>, A. Tsou<sup>3</sup>

<sup>1</sup> Department of Chemistry, State University of New York at Stony Brook, Stony Brook, NY 11794 - 3400, USA

<sup>2</sup> Department of Polymer Science and Engineering, University of Massachusetts, Amherst, MA 01003, USA.

<sup>3</sup> ExxonMobil Chemical Company, Baytown Polymers Center, TX 77522, USA

<sup>+</sup> Present address: ExxonMobil Research & Engineering Co., Annandale, NJ 08801, USA

**Summary:** Development of orientation-induced precursor structures (nuclei) prior to crystallization in isotactic polypropylene melt under shear flow was studied by *in-situ* synchrotron small-angle X-ray scattering (SAXS) and rheo-optical techniques. SAXS patterns at 165 °C immediately after shear (rate = 60 s<sup>-1</sup>, t<sub>s</sub> = 5 s) showed emergence of equatorial streaks due to oriented structures (microfibrils or shish) parallel to the flow direction and of meridional maxima due to growth of the oriented layer-like structures (kebabs) perpendicular to the flow. SAXS patterns at later times (t = 60 min after shear) indicated that the induced oriented structures were stable above the nominal melting point of iPP. DSC thermograms of sheared iPP samples confirmed the presence of two populations of crystalline fractions; one at 164 °C (corresponding to the normal melting point) and the other at 179 °C (corresponding to melting of oriented crystalline structures). Time-resolved optical micrography of sheared iPP melt (rate = 10 s<sup>-1</sup>, t<sub>s</sub> = 60 s, T = 148 °C) provided further information on orientation-induced morphology at the microscopic scale. The optical micrographs showed growth of highly elongated micron size fibril structures (threads) immediately after shear and additional spherulites nucleated on the fibrils at the later stages. Results from SAXS and rheo-optical studies suggest that a stable scaffold (network) of nuclei, consisting of shear-induced microfibrillar structures along the flow direction superimposed by layered structures perpendicular to the flow direction, form in polymer melt prior to the occurrence of primary crystallization. The scaffold dictates the final morphological features in polymer.

### Introduction

The study of polymer crystallization from melts under the influence of a flow field has drawn much interest recently<sup>[1-15]</sup> because it can provide a means to predict the product morphology and properties from varying processes. Varga and coworker<sup>[16]</sup> have shown

that in isotactic polypropylene (i-PP), melt-shearing caused development of row-nuclei in the form of microfibrillar bundles and promoted the epitaxial growth of folded chain lamellae that filled the space normal (perpendicular) to the row-nuclei, resulting in a supramolecular structure of cylindrical symmetry or cylindrites. In contrast, quiescent melt crystallization shows only spherulitic structures with folded chain lamellae. A variety of ex-situ techniques, such as TEM, optical microscopy<sup>[17-19]</sup>, etc., have been used to characterize the crystalline microstructure. However, these techniques do not address many questions concerning the structure development in a polymer melt under the imposed flow fields at the pre-crystallization stages. Various in-situ rheo-optical techniques<sup>[20-21]</sup> have been used for observation of the flow-induced structures in the early stages of crystallization. For example, Ryan<sup>[22-23]</sup> and Winter<sup>[24-25]</sup> detected, using SAXS and SALS respectively, density fluctuations prior to appearance of crystalline structures; Kornfeld<sup>[26-27]</sup> observed an upturn in birefringence in iPP polymer melt at 175 °C (above the nominal melting point) after shear. The exact nature of the oriented structure in polymer melt at high temperatures, at the early stages of crystallization, immediately after shear is the subject of interest in our laboratory.

In our previous study<sup>[28]</sup>, results of step shear experiments (rate = 57 s<sup>-1</sup>, strain = 1428% or duration of shear  $t_s$  = 0.25 s) with iPP melt at 175 °C have been reported; SAXS patterns showed meridional maxima due the growth of layer-like superstructures of crystallization precursors or primary nuclei (perpendicular to flow direction) in the polymer melt. In these experiments, under relatively weak conditions of shear fields ( $t_s$  = 0.25 s), SAXS patterns did not show an equatorial streak (indication of a microfibrillar structure). We speculated that the absence of equatorial streak may be due to low concentrations of oriented structures (microfibrils or shish) parallel to flow direction that are beyond the detection limits of our SAXS setup (> 700 Å). Under strong conditions of shear and at a lower temperature, it is expected that the concentration of oriented structures would be higher and within the detection limits of the SAXS setup, which will be chosen in this study. In addition, a separate rheo-optical study was carried out to reveal the complimentary information on structural changes at the micrometer scale. With the combined SAXS and rheo-optical results, we hope that new insights into the nature of shear-induced oriented structures (primary nuclei) in a polymer melt at the pre-crystallization stages can be revealed.

## Experimental

Ziegler-Natta i-PP homopolymers supplied by ExxonMobil Chemical Company were used in this study. The molecular weights of the iPP resin, designated as resin A, were:  $M_n = 92,000$  g/mol,  $M_w = 368,000$  g/mol,  $M_z = 965,000$  g/mol. The details of the Linkam shear apparatus and experimental procedures were given in our earlier publications<sup>[29-31]</sup>. SAXS measurements were carried out in the X27C beamline at National Synchrotron Light Source (NSLS), Brookhaven National Laboratory (BNL). A 2D MAR CCD X-ray detector (MARUSA) was employed to detect time-resolved SAXS patterns in the shear experiments. SAXS images were collected continuously: before, during, and after cessation of applied shear. The *in-situ* SAXS experimental procedures used were similar to those published previously<sup>[29-31]</sup>. The temperature protocol in the SAXS experiments was as follows:

- 1) Heat at a rate of 30 °C/min from room temperature to 200 °C.
- 2) Hold the temperature at 200 °C for 20 min.
- 3) Cool at a rate of 30 °C/min down to 165 °C.
- 4) Hold the temperature at 165 °C during x-ray measurements.

For this study, a lower temperature of 165 °C (but still higher than nominal melting point of iPP) and a strong shear field condition (rate = 60 s<sup>-1</sup>,  $t_s = 5$  s, the strain was thus about 20 times of that in  $t_s = 0.25$  s) were chosen. Corresponding WAXD measurements were also conducted to check the crystallization of the sheared melt.

*In-situ* rheo-optical experiments were performed using a Universal Polarizing Microscope (Carl Zeiss, Inc., model ZPU01) equipped with Linkam shear stage (CSS 450, similar to the one used in X-ray experiments). Morphological changes during shear-induced crystallization were followed by time-resolved optical measurements. The characteristics of temperature, shear, and experimental protocol were described in detail elsewhere<sup>[32]</sup>, which were similar to the X-ray measurements. The conditions for the rheo-optical experiment were as follows: shear rate of 10 s<sup>-1</sup>,  $t_s = 60$  s,  $T = 148$  °C. Optical micrographs were taken during crystallization of iPP melt at selected intervals after cessation of shear.

Differential Scanning Calorimetry (DSC) measurements were carried out with a Perkin-Elmer DSC-7 station. The sheared iPP sample (preserved from SAXS experiment by rapid quenching) was heated from room temperature to 200 °C at a rate of 10 °K/min.

## Results

### SAXS

Figure 1 illustrates selected typical SAXS patterns collected at 165 °C after shear (rate = 60 s<sup>-1</sup>, time of shear,  $t_s$  = 5 s). These patterns clearly show evolution of oriented structures in hundreds of angstroms in the initial stages of crystallization where no crystal reflections can be observed (this has been confirmed by separate WAXD measurements). Interestingly, under the chosen shear conditions (rather strong compared to  $t_s$  = 0.25 s), the emergence of equatorial streak is observed immediately after shear, as seen at  $t$  = 35 s. The equatorial streak can be attributed to the formation of oriented

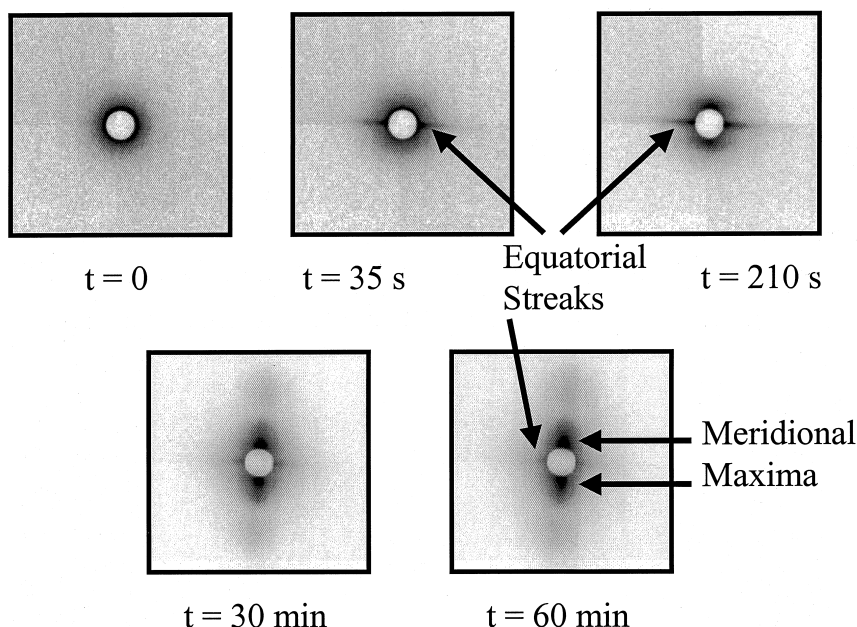


Figure 1. SAXS patterns at 165 °C before and after shear (rate = 60 s<sup>-1</sup>,  $t_s$  = 5 s)

structures (microfibrils or shish) parallel to the flow direction. Subsequently, the meridional maxima (due to layer-like oriented structures, or kebabs, perpendicular to flow direction) emerge and can be seen at  $t$  = 210 s, which become stronger at  $t$  = 30 and 60 min (these two patterns exhibit higher order reflections on the meridian).

Note that the equatorial streak is present even in the SAXS pattern at  $t$  = 60 min after shear. It appears weak in contrast to the strong meridional maxima and also because

concentration of the shish structures is expected to be much lower than concentration of the layers of kebab structures. It is also clear from the SAXS patterns, at the later stages, that the oriented structures are stable even at a temperature above the nominal melting point of iPP. The oriented structures at the later stages contain crystalline features of iPP, as verified by WAXD.

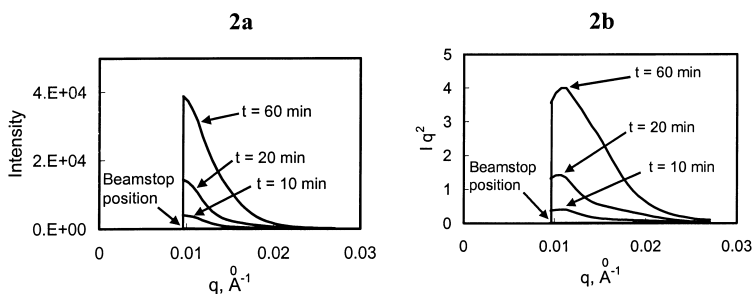


Figure 2. (a) SAXS intensity profiles along the meridian and (b) SAXS intensity profiles after Lorentz correction along the meridian, at selected times after shear in iPP melt at 165 °C (rate = 60 s<sup>-1</sup>, t<sub>s</sub> = 5 s)

SAXS intensity profiles as a function of scattering vector  $q$  along the meridian were extracted from the 2D patterns. Figure 2a shows SAXS intensity profiles along the meridian at selected times ( $t = 10, 20, 60$  min) after shear (note that SAXS intensity is very low before shear and that the intensity profile almost coincides with the x-axis). The meridional maxima is weak in the beginning; but it grows rapidly and becomes stronger at later times. It is important to note that the location of the meridian maxima is very close to the boundary of the beamstop in the current SAXS setup, which cannot be estimated in good confidence. The boundary of the beamstop corresponds to a  $q$  value of  $\sim 0.009 \text{ \AA}^{-1}$  (spacing =  $2\pi/q = 700 \text{ \AA}$ ) in the current SAXS setup. The spacing between layer-like structures is expected to be larger in the melt at higher temperatures, which would be undetectable by this SAXS setup. The Lorentz correction profiles were calculated by multiplying the SAXS intensity by  $q^2$ , which are shown in Figure 2b. Peak positions in these profiles can be clearly identified. Thus, the average spacing between the adjacent layers in the sheared iPP melt at 165 °C at the final stages is estimated to be 600 Å.

SAXS patterns in Figure 1 show emergence of equatorial streak immediately after shear which can be attributed to formation of oriented structures (microfibrils, shish or linear

nuclei) parallel to the flow direction. These initial SAXS patterns clearly suggest the presence of a large scale scaffold or network structure in sheared iPP melt, prior to the occurrence of primary crystallization. It is conceivable that the scaffold consists of bundles of chains oriented in the flow direction superimposed by the layer-like structures oriented perpendicular to flow direction. At later stages after shear, crystallization of polymer melt takes from the shish-kebab network. Detail discussions of these sequences of events are presented in the later sections.

### *Optical Microscopy*

While the SAXS experiments at high temperature provide insights into the shear-induced oriented structures in polymer melt at pre-crystallization stages on the nanometer length scale, the in-situ optical microscopy study at a lower temperature, i.e.  $T = 148\text{ }^{\circ}\text{C}$  (about  $15\text{ }^{\circ}\text{C}$  below the nominal melting point) allowed observation of the emerging morphological features on the micrometer length scale during crystallization of iPP melt. A series of optical micrographs at selected times after shear (rate =  $10\text{ s}^{-1}$ ,  $t_s = 60\text{ s}$ ,  $T = 148\text{ }^{\circ}\text{C}$ ) are illustrated in Figure 3; the formation of micron size fibrillar (thread-like) structures immediately after shear as well as emergence of the unoriented spherulitic structures at the later stages (at  $t = 300, 900\text{ s}$ ) can be clearly observed in the micrographs. The first image was taken at the instant of flow cessation (after  $60\text{ s}$  of imposed shear), where birefringent fibrils are just beginning to be formed and can be viewed on the dark field of residual amorphous melt. These fibrils are oriented parallel to the flow direction and they grow in thickness as evident from the subsequent micrograph (at  $t = 180\text{ s}$ ). At later times, additional spherulites start to grow. At even later times (several hours) spherulites cover the whole field and threads are no more visible in the microscope. The sample was left in the microscope and then was heated again. Upon heating, the spherulitic structure disappears (melts) at about  $164\text{ }^{\circ}\text{C}$  and threads become visible again in the microscope. Thread-like morphology undergoes melting at about  $175\text{ }^{\circ}\text{C}$ . This shows that threadlike morphology is preserved, stable and possesses a higher melting point, which was directly confirmed by DSC data (next section). The orientation-induced threadlike morphology has also been observed at a temperature around  $165\text{ }^{\circ}\text{C}$ , directly by heating the melt. The relationship between the melt structures prior to primary crystallization (SAXS observations at high temperatures) and the morphological features of the crystallizing polymer (microscopic observations at

lower temperatures) will be discussed later.

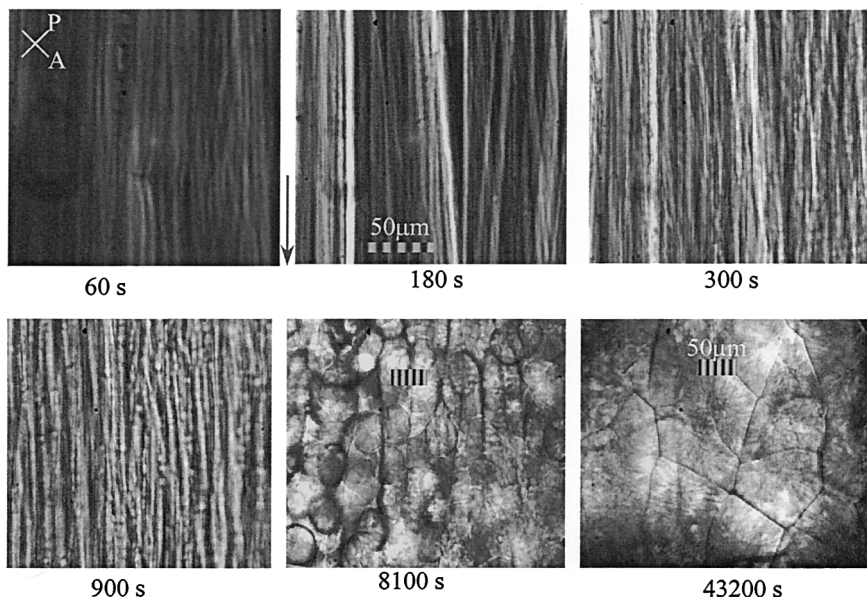


Figure 3. Optical micrographs taken at selected times during shear-induced crystallization of iPP (rate =  $10 \text{ s}^{-1}$ ,  $t_s = 60 \text{ s}$ ,  $T = 148 \text{ }^\circ\text{C}$ )<sup>[32]</sup>

### DSC

After completion of SAXS shear experiment at  $165 \text{ }^\circ\text{C}$  in the Linkam shear stage iPP was rapidly cooled to room temperature and preserved for further studies. A DSC thermogram at  $10 \text{ }^\circ\text{K/min}$  of the sheared iPP sample is shown in Figure 4. Two distinct peaks, one around  $164 \text{ }^\circ\text{C}$  (range  $150\text{--}170 \text{ }^\circ\text{C}$ ) corresponding to the nominal melting of the unoriented spherulities consisting of folded chain crystal lamellae and the other at  $179 \text{ }^\circ\text{C}$  (range  $170\text{--}185 \text{ }^\circ\text{C}$ ) that can be attributed to the melting of the oriented crystals, are clearly seen in the melting thermogram. These results indicate the presence of two populations of crystals in the crystallized polymer after shear.

### Discussion

Our interpretations of the results from SAXS, rheo-optical and DSC studies with isotactic polypropylene are presented below. They are organized to further our understanding of two aspects of orientation-induced crystallization of polymers: (1)

orientation-induced structures (nuclei) in polymer melt at the pre-crystallization stages, and (2) the subsequent morphological development in crystallizing polymer.

At the outset, it should be noted that observation of the exact nature of the melt structures (at the molecular level, i.e. polymer chain conformations) is not possible with the chosen techniques. However, the synchrotron SAXS study has provided new insights into the topography of orientation-induced structures in the polymer melt as a result of orientation and reorganization of chains due to the imposed flow field. In

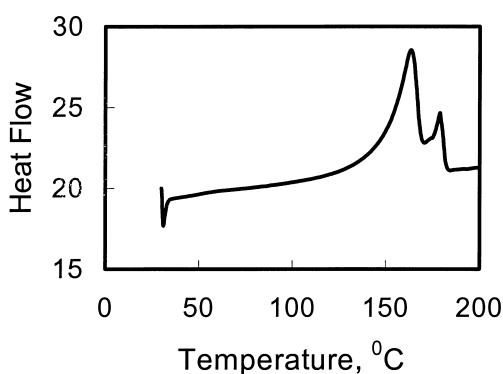


Figure 4. DSC thermogram of sheared iPP sample; heating rate = 10 °K/min

absence of a flow field (i.e., quiescent crystallization conditions), chains in the molten state are in a 'random coil' conformation and crystallization occurs in a well known fashion leading to the typical spherulitic morphology (that consists of randomly distributed chain folded crystals). Upon application of a flow field, such as shear or elongational, polymer chains orient in anisotropic molecular conformations. Observations of different morphological features in polymer bulk, such as 'shish-kebab', 'extended chain crystals', etc., can be related to the strength of the imposed flow conditions and the resultant orientation and reorganization of the chains. If the imposed field conditions are strong, as in fiber spinning, polymer chains (especially the high molecular weight species with long relaxation times) reorganize into an extended chain conformation and form a central core of extended chain crystals (shish) upon crystallization; the remaining chains (especially the low molecular weight species) can



epitaxially crystallize in the form of chain folded lamellae (kebabs) perpendicular to the shish axis. Typically, SAXS patterns of a fiber show a strong equatorial streak; its occurrence corresponds to the presence of microfibrillar crystalline structures (shish or linear nuclei). The formation of linear nuclei for interpretations of different morphologies observed in flow-induced crystallization have been proposed before by several researchers<sup>[1-3, 26-27, 33]</sup>. It is generally accepted that bundles of oriented chains arranged in a parallel conformation can form primary nucleation of extended chain crystals, which then serve as nuclei for crystallization of folded chain lamellae. However the exact nature as well as the kinetics of the formation of primary nuclei is still not clear.

Pure isotactic polypropylene melt at 165 °C (temperature of SAXS experiments) is not expected to crystallize under quiescent conditions (in a reasonable experimental time scale). The polymer melt can be considered as in a state of dynamic equilibrium, even though the chains (random coil) change conformations continuously due to thermal (Brownian) motions. After application of shear, some long relaxation time chains can remain oriented. It is thought that this reorganization creates regions of different electron density with sufficient contrast that can be detected by SAXS. Immediately after shear, the sheared melt at a temperature above the nominal melting point can be considered as in a “pre-crystallization” stage. Thus, the initial SAXS patterns (in Figure 1) provide a topography of the melt structure before crystallization. We describe below a possible sequence of dynamic events during orientation-induced crystallization.

The immediate and primary effect of the applied shear is orientation of chain segments of molecules towards the direction of the flow. The segmental molecular orientation promotes disentanglement and creates bundles of aligned chain segments in the melt. Equatorial streaks observed in the SAXS pattern at  $t = 35$  s (first frame after shear) suggest that linear structures in tens of angstroms oriented parallel to the flow direction form within a very short period of time (matter of few seconds) after application of shear and that they have higher electron density than the isotropic melt. These structures presumably consist of bundles of chain segments arranged in a parallel array, like a thin microfibril or shish. It is expected that the long chains (from high molecular weight fraction) attain higher degree of orientation and alignment in flow. Also, since the stability of the oriented chains is governed by the relaxation behaviour of polymer molecules; the longer chains take a longer time for relaxation from deformation than

shorter ones, and therefore can remain oriented longer after cessation of flow. In other words, the oriented long chains do not relax and they form coalescence (or bundles) of adjacent chain segments with lower free energy. These serve as precursors or linear nuclei for crystallization of the extended chain crystals in microfibrillar form.

It should be emphasized here that it is not possible to determine the exact nature of the linear nuclei with the current SAXS (and WAXD) setup. The equatorial streaks in the SAXS patterns at the initial stages could also be due to the formation of actual crystalline entities at the initial stages of crystallization after shear instead of the non-crystalline precursor structures described earlier. If the shish structure is crystalline, the total crystallinity must be below the detection limit of WAXD (1%) since no crystal reflection signals were detected. It is our opinion that the formation of the non-crystalline precursor phase in i-PP is quite possible. This is because the i-PP chains adopt 3 chain helical conformations (there are four types of helices in i-PP: left- and right-handed helices as well as 'up' and 'down' helices concerning the pending  $\text{CH}_3$  group), which must be organized in a specific spatial arrangement to form the  $\alpha$ -monoclinic nucleus. This is not so easy to accomplish by stretching the chains with random assembly of helical hands. On the other hand, in the case of linear polyethylene, it is conceived that crystalline nuclei could form immediately upon alignment of chains. In polyethylene, the equatorial streaks in SAXS patterns, obtained immediately after shear at high temperature (near polymer melting point) should arise from the crystalline structures. In view that the total volume fraction of the orientation-induced 'nuclei' should be larger than 1%, we believe that the existence of both crystalline or non-crystalline nuclei in iPP is possible. Recently, a rheological study carried out by Winter et al. [34] has showed that the gelation behavior exists in the crystallizing iPP melts before crystallization, which supports the presence of a connected network made of 'nuclei'. In addition, the phenomenon of self-nucleation [35, 36], well known in the polymer crystallization field, is also consistent with the above findings

Subsequently, meridional maxima were observed in SAXS patterns, as can be seen in the image at  $t = 210$  s (Figure 1). The meridional maxima suggest emergence of oriented structures arranged perpendicularly to the flow direction. These structures are presumed to grow epitaxially from several locations along the central core (linear nuclei). In a way, they are similar to the layered structures observed during crazing of the polymer solid upon deformation, except that no microvoids are involved in the sheared melt. It is

our opinion that the observed kebab structures are probably folded chain crystals, which will facilitate the development of folded chain lamellae oriented perpendicular to the flow direction. Thus, initial SAXS patterns of iPP melt at 165 °C after shear suggest that a scaffold or network of oriented structures (crystalline and non-crystalline nuclei), consisting of bundles of parallel chains in flow direction superimposed by layers of oriented crystalline structures perpendicular to flow direction, form in the melt prior to primary crystallization. The final spacing between the layered structures in iPP at 165 °C under the chosen conditions of shear was about 600 Å (Figure 2).

The development of nuclei network in polymer melt after shear appears to be very fast - the equatorial streak was observed in the first SAXS image (at  $t = 35$  s) and the meridional maxima emerge soon afterwards (clearly seen at  $t = 210$  s). It is quite possible that the meridional maxima may have been initiated at the earlier stage, i.e. before  $t = 210$  s, but could not be resolved due to limitations of the current SAXS setup. In Figure 1, SAXS patterns at the later stages ( $t = 30, 60$  min) show development of stable shish and kebab structures. These structures contain the  $\alpha$ -form crystals (as verified by WAXD) and are stable even at a temperature near the original nominal melting point. In fact, we have demonstrated that the shear-induced structures are stable at 175 °C that is about 10 °C above the nominal melting point in a previous study<sup>[31]</sup>. DSC results of the sheared iPP sample also confirmed the presence of high melting shear-induced crystals. In Figure 4, the DSC thermogram clearly shows that a new endotherm is induced by shearing, which occurs at about 15 °C above the nominal melting point of iPP crystallized in the quiescent state.

It is expected that the final morphology of solid polymer would be directly governed by the structures formed in the melt in the initial stages of crystallization. Optical microscopy study of crystallization of sheared iPP melt provide some insights into these structures at the pre-crystallization stages. As mentioned earlier, the spherulitic morphology is formed under quiescent crystallization conditions, while a cylindrite morphology is formed under flow conditions. It should be noted that optical micrographs show morphological features on a larger length scale. The features of shear-induced fibrils (threads) become visible when the diameter is above 1  $\mu\text{m}$  and higher. The large diameter of these fibrils suggests that each fibril should contain several shish-kebab assemblies. Keller et al. have demonstrated that for polyethylene, each shish-kebab assembly has a diameter in the range of 30-100 nm under extensional

flow<sup>[1]</sup>. The fibrillar structures observed in the initial stages by optical microscopy are consistent with the morphology of cylindrites<sup>[16]</sup>. In Figure 3, it is seen that spherulites are formed at later times ( $t = 300$  s). From WAXD study, we find that some spherulites contain  $\beta$ -form crystals (which is presumed to grow from shorter chains and nucleated by the oriented  $\alpha$ -form crystals), that are consistent with our previously reported WAXD observations<sup>[30]</sup> of sheared iPP melt at lower temperatures (140 °C).

## Conclusions

In-situ SAXS study of sheared iPP melt at a temperature near its nominal melting point provided some new insights into the topography of shear-induced structures in a polymer melt at the pre-crystallization stages. SAXS patterns taken immediately after shear showed that a space-filling scaffold or network of nuclei, consisting of bundles of chains oriented in the flow direction (linear nuclei, microfibrillar or shish) and layers of relaxed chain-folded crystalline superstructures (kebabs) oriented perpendicular to the flow direction form in the melt in the initial stages of crystallization. The linear nuclei may contain both crystalline and non-crystalline entities. The combined SAXS and WAXD results at later times after shear indicated that these shish-kebab structures are predominant crystalline. DSC results confirmed that the shear-induced crystalline structures have a melting point about 15 °C above the nominal melting temperature of iPP. We believe that the space-filling network of primary nuclei in polymer melt at the pre-crystallization stages determines the final morphological features in bulk of solid polymer. The process of network formation is very fast, almost immediately after shear.

## Acknowledgement

The financial support of this work was provided by NSF (DMR-0099804) and ExxonMobil Company. The authors also thank Prof. Richard S. Stein for valuable comments. We acknowledge the assistance of Drs. Fengji Yeh, Lizhi Liu, Dufei Fang and Shaofeng Ran for synchrotron experiments setup.

[1] A. Keller, H. W. H. Kolnaar, „*Proc. Polym. in Mat. Sci. & Techn. Vol. 18*” Meijer H.E.H. Ed., John Wiley & Sons 1997, p. 189.

[2] G. Eder, H. Janeschitz-Kriegl, „*Proc. Polym. in Mat. Sci. & Techn. Vol. 18*” Meijer H.E.H. Ed., John Wiley & Sons 1997, p. 268.

[3] G. Eder, H. Janeschitz-Kriegl; S. Liedauer, *Prog. Polym. Sci.*, **1990**, *15*, 629.

[4] S. Liedauer, G. Eder, H. Janeschitz-Kriegl, *Intern. Polym. Process.*, **1995**, *10*, 243.

[5] A. Keller, M. Hikosaka, S. Rastogi, *Phys. Sci.*, **1996**, *T66*, 243.

- [6] A. Keller, M. Hikosaka, S. Rastogi, A. Toda, P. J. Barham, G. Goldbeck-Wood, *J. Mater. Sci.*, **1994**, 29, 2579.
- [7] A. Keller, S. Z. D. Cheng, *Polymer*, **1998**, 39, 4461.
- [8] K. Kobayashi, J. Nagasawa, *J. Macromol. Sci., Phys. B*, **1970**, 4, 331.
- [9] G. Kalay, M. J. Bevis, *J. Polym. Sci., Polym. Phys.*, **1997**, 35, 265.
- [10] U. Goschel, F. H. M. Swartjes, G. W. M. Peters, H. E. H. Meijer, *Polymer*, **2000**, 41, 1541.
- [11] H. Janeschitz-Kriegl, *Colloid Polym. Sci.*, **1997**, 275, 1121.
- [12] H. Janeschitz-Kriegl, E. Tatajski, H. Wippel, *Colloid Polym. Sci.*, **1999**, 277, 217.
- [13] G. Strobl, *Eur. Phys. J. E.: Soft Mat.*, **2001**, in press.
- [14] B. Heck, T. Hugel, M. Iijima and G. Strobl, *Polymer*, **2000**, 41, 8839.
- [15] Z. Wang, B. S. Hsiao, E. B. Sirota, P. Agarwal, S. Srinivas, *Macromolecules*, **2000**, 33, 978.
- [16] J. Varga, J. Karger-Kocsis, *J. Polym. Sci., Part B: Polym. Phys.*, **1996**, 34, 657.
- [17] Tribout, C.; Monasse, B.; Haudin, *Colloid Polym. Sci.*, **1996**, 274, 197.
- [18] B. Monasse, *J. Mater. Sci.*, **1995**, 30, 5002.
- [19] C. Duplay, B. Monasse, J. Haudin, J. Costa, *Polym. Int.*, **1999**, 48, 320.
- [20] T. Hashimoto; T. Takebe; S. Suehiro, *Polym. J.*, **1986**, 18, 123.
- [21] J. Lauger, W. Gronski, *Rheol. Acta*, **1995**, 34, 70.
- [22] A. J. Ryan, N. J. Terrill, J. P. A. Fairclough, in "Scattering of Polymers", P. Cebe, B. S. Hsiao, D. J. Lohse Eds., ACS Symp. Ser. 739, Oxford, Washington D.C. 2000, p. 201.
- [23] N. J. Terrill, J. P. A. Fairclough, E. Towns-Andrews, B. U. Komanschek, R. J. Young, A. J. Ryan, *Polymer*, **1998**, 39, 2381.
- [24] N. V. Pogodina; H. H. Winter, *Macromolecules*, **1998**, 31, 8164.
- [25] N. V. Pogodina, S. K. S. Siddiquee; J. W. VanEgmond; H. H. Winter, *Macromolecules*, **1999**, 32, 1167.
- [26] G. Kumaraswamy, A. M. Issaian, J. A. Kornfield, *Macromolecules*, **1999**, 32, 7537.
- [27] G. Kumaraswamy, R. K. Varma, A. M. Issaian; J. A. Kornfield, F. Yeh, B. S. Hsiao, *Polymer*, **2000**, 41, 8931.
- [28] R. H. Somani, B. S. Hsiao, A. Nogales, S. Srinivas, A. Tsou, I. Sics, F. Balta-Calleja, T. A. Ezquerria, *Macromolecules*, **2000**, 33, 9385.
- [29] A. Nogales, B. S. Hsiao, R. H. Somani, S. Srinivas, A. Tsou, F. Balta-Calleja, T. A. Ezquerria, T. A., *Polymer*, **2000**, 42, 5247.
- [30] R. H. Somani, B. S. Hsiao, A. Nogales, S. Srinivas, A. Tsou, F. Balta-Calleja, T. A. Ezquerria, *Macromolecules*, **2001**, 34, 5902.
- [31] R. H. Somani, L. Yang, B. S. Hsiao, *Physica A*, **2001**, in press.
- [32] N. V. Pogodina, V. P. Lavrenko, S. Srinivas, H. H. Winter, *Macromolecules*, **2001**, 42, 9031.
- [33] J. T. Judge, R. S. Stein, *J. Appl. Phys.*, **1961**, 32, 2357.
- [34] N. V. Pogodina, H. H. Winter, *Macromolecules*, **1998**, 3, 938.
- [35] W. Banks, M. Gordon, A. Sharples, *Polymer*, **1963**, 4, 289.
- [36] D. C. Basset, A. Keller, *Philos. Mag.*, **1962**, 7, 1553.